Role of aquaporin-4 water channel in the development and integrity of the blood-brain barrier

Beatrice Nico[1,*], Antonio Frigeri[2], Grazia Paola Nicchia[2], Fabio Quondamatteo[3], Rainer Herken[3], Mariella Errede[1], Domenico Ribatti[1], Maria Svelto[2] and Luisa Roncali[1]

[1]Department of Human Anatomy and Histology and [2]Department of General and Environmental Physiology, University of Bari Medical School, I-70124 Bari, Italy
[3]Zentrum Anatomie, Abteilung Histologie, Universitat Gottingen, D-37075 Gottingen, Germany
*Author for correspondence (e-mail: nico@histology.uniba.it)

SUMMARY

In this study, we have investigated the expression of aquaporin 4 during blood-brain barrier development in the optic tectum of chick embryos and newly hatched chicks, by means of western-blot, reverse transcriptase-polymerase chain reaction, immunohistochemistry, and freeze-fracture and high-resolution immunogold electron microscopy.

In the optic tecta of day-14 embryos, western blot analysis revealed an approx. 30 kDa band, immunoreactive for aquaporin-4, which was increased in day-20 embryos and in chicks. Semi-quantitative reverse transcriptase chain reaction experiments showed that there was already a high level of aquaporin-4 mRNA in day-9 embryos as well as in the subsequent stages and in newly hatched chicks. Immunohistochemically, reactivity for aquaporin-4 was detected in the optic tectum of day-14 embryos; similar results were obtained in telencephalon and cerebellum. Ultrastructurally, the microvessels of the tectum showed immunoreactivity for aquaporin-4 on the astroglial endfeet, which discontinuously surrounded endothelial cells joined by immature tight junctions. In the tectum, telencephalon and cerebellum of 20-day embryos and chicks, aquaporin-4 strongly labeled the ependymal cells and the subpial glial membranes, as well as the bodies and processes of astroglial cells. A continuous aquaporin-4 staining was found around the microvessel endothelial cells, which were sealed off from one another by extensive tight junctions. A complete astrocytic sheath, labeled by anti-aquaporin-4 gold particles, enveloped the endothelium-pericyte layer. Orthogonal arrays of particles were observed on fractured astrocytic membranes, starting from embryonic day 14 when the aquaporin-4 immunogold staining revealed clusters of gold particles, often forming square or rectangular clusters. The results showed that aquaporin-4 expression and organization of the intramembrane particles in orthogonal arrays followed the same temporal sequence.

Finally, the lipopolysaccharide, a substance that induces blood-brain barrier distruption, determines a remarkable reduction in aquaporin-4 labeling, expressed by a few aquaporin-4 gold particles attached on swollen perivascular glial membranes.

All these data show that aquaporin-4 expression occurs in the chick embryonic brain, in parallel with maturation and functioning of the blood-brain barrier and suggest that there is a close relationship between water transport regulation and brain development.

Key words: Aquaporin, Blood-brain barrier, Chick embryo, Glial cell, Lipopolysaccharide

INTRODUCTION

Membrane water transport is mediated by a family of molecular water channels, called aquaporins (AQPs), which have been identified in the epithelial and endothelial cells of higher vertebrates (Verkman et al., 1996; Agre et al., 1998; Nielsen et al., 1993; Nielsen and Agre, 1995). The presence of a specific AQP, namely AQP4, has been demonstrated in the rat brain (Hasegawa et al., 1994; Jung et al., 1994), where it is highly expressed in a polarized way by ependymoglial cells and by perivascular processes of astrocytes, in orthogonal arrays of intramembrane particles (OAPs) (Frigeri et al., 1995b; Yang et al., 1995; Nielsen et al., 1997; Verbavatz et al., 1997; Rash et al., 1998).

Astrocytes function in the blood-brain barrier (BBB), a complex glio-vascular system that controls the Central Nervous System (CNS) homeostasis, preventing the non-specific passage of hydrophilic solutes between blood and neuropile. Moreover, morphological and biochemical features of brain capillaries, including endothelial tight junctions and membrane carriers, selectively regulate nutrient transport in the brain, ensuring neuronal protection (Reese and Karnowsky, 1967; Betz and Goldstein, 1986; Pardridge, 1988). Astrocytes are considered inducers of the barrier properties of the endothelium as well as of its permeability properties (DeBault and Cancilla, 1980; Cancilla and DeBault, 1983; Beck et al., 1984; Janzer and Raff, 1987; Tao Cheng et al., 1987; Meresse et al., 1989; Rubin et al., 1991; Raub et al., 1992; Sun et al., 1995). BBB also controls water transport, which is very important in CNS physiology because it is involved with CSF production, fluid transport across the endothelium and osmolality compensation in potassium siphoning (Nagelhus et al., 1998; Nagelhus et al., 1999; Walz and Hinks, 1985; Newman, 1995).

During embryonic life, BBB differentiation is a gradual process that leads to embryonic vessels acquiring barrier properties through progressive decrease in permeability and expression of specific endothelial transporters and antigens (Saunders, 1977; Risau and Wolburg, 1990), and one of the most debated questions concerning the BBB differentiation is the time course of its maturation. In birds, the precocious brain development is associated with the BBB being already structurally and functionally developed in embryonic life (Wakai and Hirokawa, 1978; Roncali et al., 1986), which is different from rodents where the BBB is only completely differentiated and functioning in postnatal life (Schulze and Firth, 1992).

The developmental expression of aquaporin proteins is complex and little known (King et al., 1997). Recently, Wen et al. (Wen et al., 1999) demonstrated that AQP4 expression in the rat cerebellum is post-natal, suggesting a lack of water flux regulation in the embryonic brain, whereas other aquaporins such as AQP1 are expressed in the respiratory tract at the end of the embryonic life. Here, we tested the hypothesis that expression of AQP4 in brain is functionally related to the maturation and integrity of the BBB. We studied the developmental expression of AQP4 protein in the optic tectum of chick embryos by (1) quantitative western blot and RT-PCR analysis; (2) light immunocytochemistry; and (3) immunogold-electron microscopy. The developmental expression of AQP4 protein was compared with the formation of OAPs in the perivascular astrocytic membrane, utilizing freeze-fracture techniques. The optic tectum was chosen as our main model of study since vessel development and BBB differentiation been investigated here in detail by various morphofunctional approaches (Roncali et al., 1986; Bertossi et al., 1993; Nico et al., 1994; Nico et al., 1997), and immunocytochemical expression of AQP4 in the telencephalon and cerebellum have also been reported.

With the aim of further clarifying the biological role of AQP4 during BBB development, we studied the expression of AQP4 in the optic tectum of chicken embryos subjected to treatment with lipolysaccharide (LPS), which mimics the BBB distruption in meningoencephalitis (Quagliarello et al., 1986) and provokes severe brain oedema. The BBB integrity was evaluated by intravascular injection of horseradish peroxidase (HRP), a marker of the vascular permeability, in 20-day embryos in which the BBB is morphofunctionally well developed (Roncali et al., 1986).

The results taken as a whole demonstrate that the AQP4 protein is expressed in embryonic chick brain by astroglial cells, and that this expression paralles the vessel endothelial differentiation, the perivascular arrangement of astrocyte processes and the development of OAPs on their plasma membranes. Moreover, the observed deficiency in AQP4 expression revealed in the brain oedema following the LPS treatment suggests that regulation of water flux in embryonic life is tightly coupled both to the differentiation and the functioning of the BBB.

MATERIALS AND METHODS

Morphology
Animals
Experiments were performed on chick embryos from fertilized White Leghorn chicken eggs incubated from the start of embryogenesis under conditions of constant humidity at 37°C. We used 200 embryos.

SDS-PAGE and western blot analysis
10 of each of day-3, -9, -14 and –20 chick embryos and 2-day-old chicks were sacrificed by decapitation. Optic tecta were isolated from the brains, minced finely and homogenized in ice-cold buffer containing 300 mM mannitol, 12 mM Hepes-Tris, pH 7.4, and protease inhibitors (1 µg/ml leupeptin, 1 µg/ml pepstatin and 1 mM PMSF). After homogenization in a Potter apparatus and centrifugation at 1000 g for 10 minutes, a low speed pellet was prepared by centrifugation at 17000 g for 45 minutes. The membrane pellet was then resuspended in mannitol buffer and protein content measured using the modified Lowry procedure (Markwell et al., 1978). For SDS-PAGE, samples (50 µg/lane) were solubilized in Laemli buffer, heated at 37°C for 10 minutes and resolved on a 13% polyacrylamide gel: two gels were prepared in parallel. One was stained with Coomassie Blue and the other was subjected to immunoblotting. The proteins were electrotransferred to a PVDF membrane (Millipore, Bedford, MA, USA) and immunoblotting was performed as previously described (Frigeri et al., 1998). Briefly, the membrane with blotted proteins was blocked with Blotto containing 5% non-fat dry milk for 1 hour and incubated for 2 hours with serum anti-AQP4 diluted 1:1000. Polyclonal antibodies against the C terminus of AQP4 (amino acids 287-301, EKGKDSSGEVLSSV) were raised in rabbit as described previously (Frigeri et al., 1995a). After four washings with blocking buffer, the membrane was incubated for 1 hour with peroxidase-conjugated goat anti-rabbit antibody (Sigma, Chemical Co., St Louis, MO, USA) diluted 1:5000 in blocking buffer, washed again, and peroxidase activity revealed by chemiluminescence (BM chemiluminescence Western blot kit, Boehringer-Manheim, Gmbh, Germany). Control experiments were performed using immunodepleted antibodies as previously reported (Frigeri et al., 1995a; Frigeri et al., 1995b).

Coomassie-stained gels and ECL film were scanned using UMAX SPEED IIC scanner and Adobe Photoshop software (Adobe, San Jose, Ca, USA). Densitometry analysis was performed using Scion Image software (Scion, Scion Inc., Frederick, MD, USA) and AQP4 protein levels at different developmental stages were expressed as a fraction of the respective adult level. Differences in the protein loading detected by densitometric analysis were taken into account for the determination of AQP4 protein level.

Quantitative RT-PCR
Total RNA was prepared from optic tecta of day-3, -9, -14 and -20 embryos and 2-day-old chicks using the Trizol reagent (Gibco-Life Technologies, Gaithersburg, MD, USA) and cDNAs were generated from 5 µg of total RNA using M-MLV reverse transcriptase (Superscript II, Gibco) and random primers. The cDNAs were used to amplify, by PCR, a 340 bp fragment using specific primers for the AQP4 sequence (forward 5′-ATCAGCGGTGGCCACATCAA-3′; reverse 5′-TCCAATTGCAACAGAAAACC-3′). The relative amount of AQP4 transcript was estimated by direct comparison between multiple samples after standardization with co-amplification of 18S rRNA (Quantum RNA kit, Ambion, San Jose, Ca, USA). For quantification, the PCR products were subjected to electrophoresis in a 1% agarose gel and stained with ethidium bromide. Photographs were taken with a polaroid camera and the positive films scanned. Densitometric analysis was performed as described for western blot films and the data presented as the AQP47 18S RNA ratio.

Control series
Fixation and preparation of tissue
Small pieces of optic tectum, telencephalon and cerebellum from chick embryos incubated for 9, 14 and 20 days and from 2-day-old chickens were fixed (1) in 0.1 M phoshate-buffered 3% glutaraldehyde solution for conventional electron microscopy and freeze-fracture studies; (2)

in a modified acetate-free Bouin fluid for immunohistochemistry investigation at the light microscopical level; or (3) in 0.1 M phosphate-buffered 0.5% glutaraldehyde for immunoelectron microscopic study.

Conventional electron microscopy

The specimens were post-fixed with 1% osmium tetroxide, dehydrated in an ascending ethanol series and embedded in Epon 812. Semithin sections were cut for orientation purposes and stained with Toluidine Blue. Thereafter, ultrathin sections of 60 nm were cut with a diamond knife on an LKB V ultratome, stained with uranyl acetate and lead citrate and examined with a Zeiss EM 109 (Zeiss, Oberkochen, Germany) electron microscope. In all cases, at every stage, 30 ultrathin sections were observed.

Freeze-fracture

Small fragments of optic tecta from chick embryos incubated for 14 and 20 days and from chicks were rinsed in 0.1 M phosphate buffer and passed through a cold glycerol series (10%-20%-30%) for 30 minutes. They were then placed in a drop of glycerol on specimen discs and frozen in liquid nitrogen-cooled freon-22. Platinum replicas were prepared in a Balzers BAF 400 Freon-Etch Unit (temperature $-118°C$, with a vacuum of 5×10^{-6} mbar). The replicas (20 in all cases, at every stage) were cleaned free of adhering tissue in a 6% sodium hypochlorite solution for 1 hour, washed in methanol, then in water, mounted on 200 mesh copper grids and examined in a Zeiss EM 109 electron microscope. Plasma membrane fracture faces were designated P and E according to Branton et al. (Branton et al., 1975).

Immunohistochemistry

Light microscopy

The specimens were dehydrated in an ascending ethanol series and embedded in paraffin. Coronal sections of 5 μm were collected on polylysine-coated slides, deparaffinized, rehydrated and rinsed for 10 minutes in Tris-buffered saline (TBS), pH 7.2. Endogenous peroxidase was blocked by incubation in 3% H_2O_2 dissolved in methanol for 45 minutes in the dark. Each of the following steps was carried out at room temperature and followed by rinsing for 10 minutes in TBS. The sections (50 in all cases, at every stage) were treated with 1% bovine serum albumin in TBS for 10 minutes and then sequentially incubated with (1) primary rabbit anti-AQP4 antibody diluted 1:10 in TBS overnight at 4°C; (2) secondary antibody, goat anti-rabbit (Dakopats) diluted 1:50 in TBS for 30 minutes at room temperature, followed by the PAP complex, using commercial reagents (Dakopats, Hamburg, Germany). Finally, the sections were treated with 0.06% 3,3′ diaminobenzidine in Tris-HCl buffer in the presence of H_2O_2, counterstained with Mayer's hematoxylin for 1 minute and mounted in buffered glycerin. Moreover, some sections were incubated with the primary antibody using a three-step biotin-avidin-peroxidase system. As secondary antibody we used a biotin-labeled swine anti-rabbit IgG (Vector Inc., Burlingame, CA, USA) followed by streptavidin-peroxidase conjugate (Vector Inc.). The developing reaction was performed in 0.05 M acetate buffer, pH 5.1, 0.02% 3-amino-9-ethylcarbazole grade II (Sigma Chemical Co.) and 0.05% H_2O_2. Sections were then washed in the same buffer, counterstained and mounted as previously described. Negative controls, obtained by substituting normal rabbit serum for the primary antibody, showed no staining of the sections.

Immunogold electron microscopy

Small pieces of brain cortex were fixed in a 0.1 M phosphate-buffered mixture of 0.1% glutaraldehyde for 30 minutes at 4°C and then rinsed with 10 mM ammonium chloride in 0.1 M phoshate-buffered saline PBS for 45 minutes. The samples were dehydrated in an ascending ethanol series and embedded in the acrylic resin LR-Gold (London Resin Co., Reading, UK) with 0.8% benzil. The resin was hardened at –25°C under the light of a halogen lamp (500 W). Thin sections

were cut with an LKB V ultramicrotome and collected on formvar-coated nickel grids. The grids were incubated for 10 minutes at room temperature with TBS buffer. Unspecific reactions were blocked with 1% BSA-TBS, pH 7.4, for 10 minutes, at room temperature. The sections (30 for all cases at every stage) were incubated with the primary anti-AQP4 antibody at room temperature overnight, washed with TBS, and incubated for 1 hour at room temperature with the second antibody (goat anti-rabbit) coupled to 6 nm gold particles (Chemicon Intern. Inc.). After washing with TBS, the grids were stained with 1% uranyl acetate, followed by 1% lead citrate and examined with a Zeiss EM 109 electron microscope.

Experimental series

For testing the AQP4 biological role, a group of 20 embryos was treated on day 19 with 1 μg/ml bacterial LPS (from *Escherichia coli*,
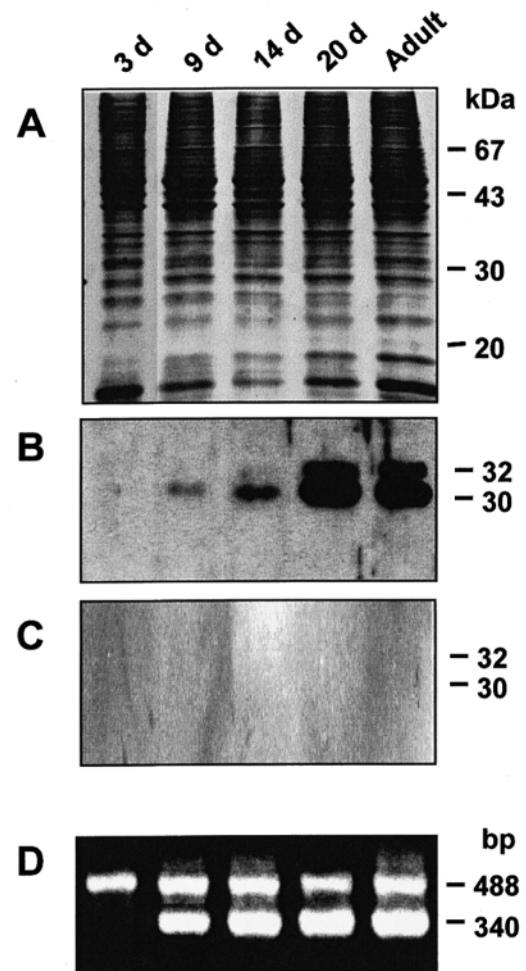
Fig. 1. Analysis of AQP4 protein and mRNA levels in the avian optic tectum. Optic tecta homogenates from chick embryos (day 3, 9, 14, 20) and 2-day-old chicks were electrophoresed on 13% gels under reducing conditions and stained with Coomassie Blue. (B) Western blot analysis of AQP4 protein revealed by chemiluminescence. (C) Western blot experiment performed using immunodepleted antibodies obtained with affinity-purified antibodies pre-incubated with the specific AQP4 peptide used for the immunization. Note that the absence of the staining demonstrates the specificity of the results shown in A. (D) Quantitative RT-PCR experiments. The 488 bp band corresponds to the 18S RNA internal standard, whereas the 340 bp band corresponds to the AQP4-specific PCR product. The positions of marker proteins (kDa) or RNAs (bp) are shown.
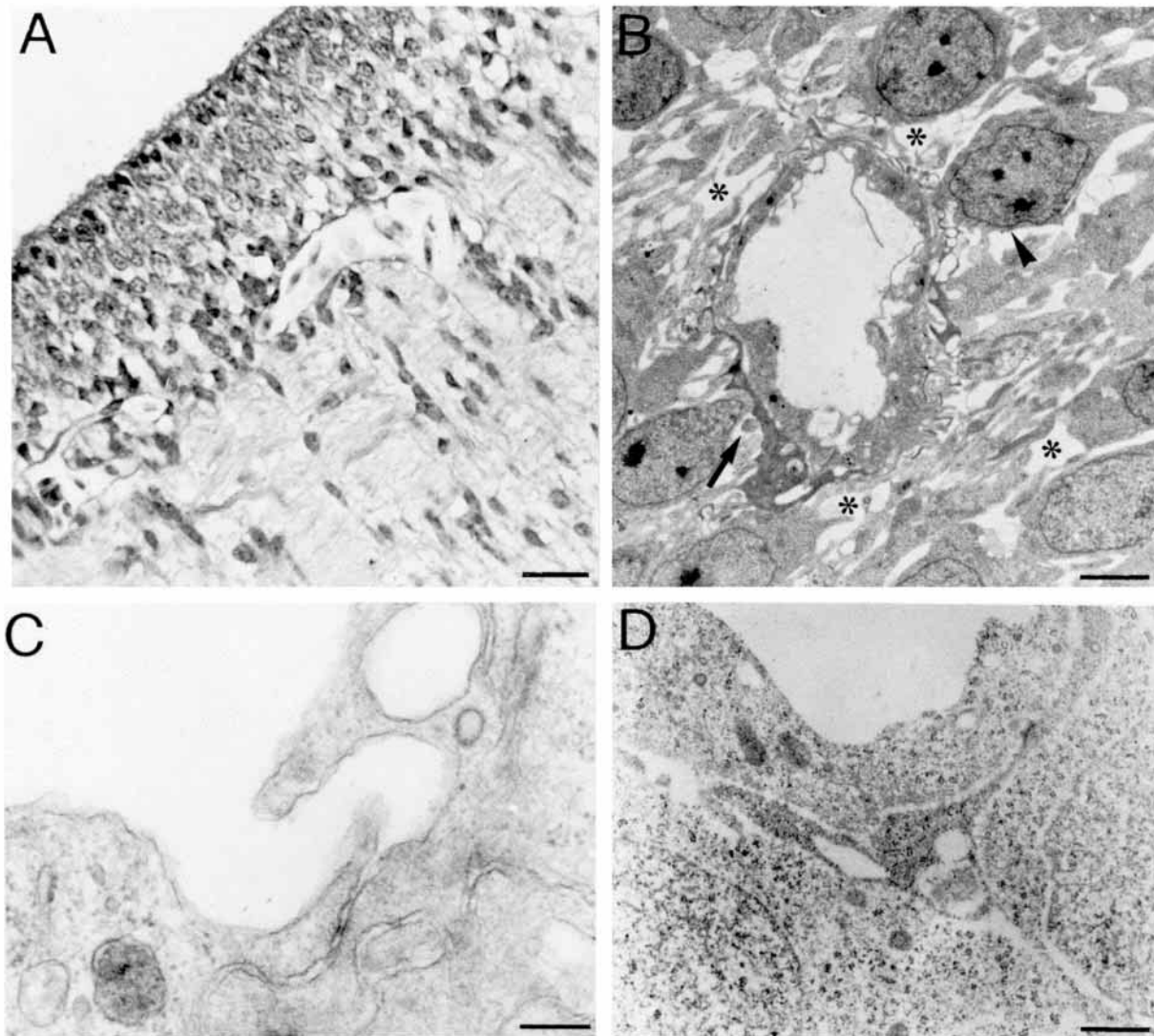
Fig. 2. Morphological features in day-9 embryos. (A) Optic tectum section showing unstained microvessel walls and neuropile after light microscopical immunodetection of AQP4. (B) A microvessel is lined by irregular endothelium and surrounded by pericytic processes (arrow). Large perivascular spaces (asterisks) and neuroblasts (arrowhead) are recognizable around the microvessel. (C) Terminal ends of contiguous endothelial cells are simply apposed and show intercellular clefts devoid of tight junctional systems. (D) Part of an unlabeled vessel after immunogold electron microscopic detection of AQP4. Scale bars, 25 µm (A); 2 µm (B); 0.18 µm (C); 0.4 µm (D).

serotype 055.B5, Sigma Co., St Louis, MO, USA) injected subcutaneously. Comparable LPS concentration and time of exposure have been found to increase BBB permeability both in vivo (Wilspelwey et al., 1988) and in vitro (Tunkel et al., 1991). On day 20, optic tecta were processed for: (1) HRP assay, (2) conventional electron microscopy, (3) AQP4 immunohistochemistry and immunogold electron microscopy.

HRP assay

The embryos received an intracardial injection of HRP (0.3 mg Sigma type II HRP per gram body mass in 0.1 ml saline solution). After 5 minutes the embryos were decapitated and the optic tecta were fixed by immersion in 3% glutaraldehyde in 0.1 M sodium cacodylate buffer (pH 7.3) for 3 hours at 4°C and then washed in the same buffer for 12 hours. 50 µm sections were cut with a vibratome and incubated for 30 minutes at room temperature in a 0.05% solution of 3.3′-diaminobenzidine in 0.05 M Tris-HCl buffer (pH 7.6) containing 0.01% H_2O_2. After incubation, some of the slices were dehydrated, mounted on slides and examined on a SM Leitz Dialux 20

photomicroscope (Leitz, Wetzlar, Germany). Other sections were post-fixed in 1% osmium tetroxide for 1 hour, dehydrated in a graded ethanol series and embedded in Epon 812 for electron microscopic evaluation. Semithin sections were cut with an LKB V ultramicrotome and stained with 1% Toluidine Blue. Ultrathin sections were cut with an LKB V ultramicrotome, stained with lead citrate and examined with a Zeiss EM109 electron microscope. Control optic tecta injected only with saline solution, were subjected to the same procedures.

Conventional electron microscopy, immunohistochemistry and immunogold electron microscopy were performed following the same procedures as described for the control series.

RESULTS

Western blot and RT-PCR analysis

In order to analyze the expression of AQP4 in avian brain and its developmental pattern we first performed western blot and
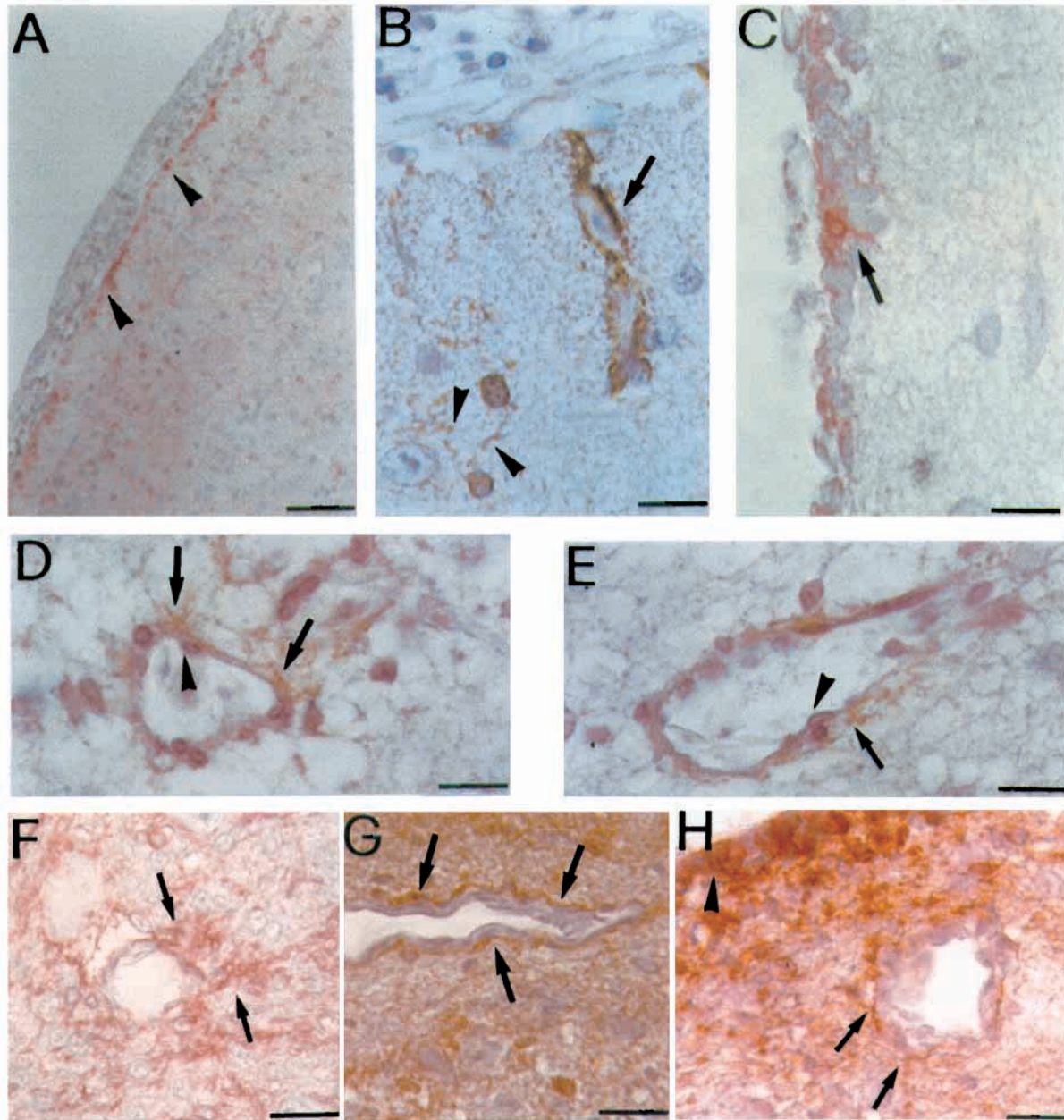
Fig. 3. Immunohistochemical features in day-14 embryos (A-E); day-20 embryos (F-G) and 2-day-old chicks (H). Light microscopic immunodetection of AQP4 in optic tecta processed by the biotin-avidin peroxidase method (A,C,F) and PAP-DAB method (B,D,E,G,H). (A,B) Glia limiting membrane (A, arrowhead) and a microvessel growing into the wall of the CNS anlage (B, arrow) immunostained for AQP4. Note in B a fine labeling of glial processes in the neuropile (arrowheads). (C) The ventricular epithelium shows a labeled body and process of an ependymoglial cell (arrow) between unlabeled cells. (D,E) Bodies and processes (arrows) of astroglial cells surround microvessel walls discontinuously. Note the unlabeled endothelium (arrowhead). (F-H) Light microscopic immunodetection of AQP4 in bodies and processes of astrocytes, which are localized in the neuropile and envelop blood vessels completely (arrows). Note in H the ependymal cells stained for AQP4 (arrowhead) and an astrocytic process (arrow) sheathing a microvessel of the tectum subependymal layer finely labeled for AQP4. Scale bars, 50 μm (A); 10 μm (B,D-F,H); 16 μm (C); 40 μm (G).

RT-PCR experiments. Coomassie Blue-stained gels showed that the overall protein band patterns in the embryo and adult chicks were substantially similar (Fig. 1A). Immunoblot analysis revealed that the immunoreactive AQP4 protein starts to be detectable in day-9 embryos and progressively increases, reaching the highest level in day-20 embryos (Fig. 1B). As in rat, two bands of 30 and 32 kDa were detected and corresponded to the splice variants of AQP4 protein indicated

in a previous study (Jung et al., 1994; Neely et al., 1998; Nicchia et al., 2000). Densitometric analysis revealed the 32 kDa AQP4 band, corresponding to 25% of the total amount of AQP4 protein. The specificity of the result was confirmed using immunodepleted antibodies (Fig. 1C). AQP4 was expressed at low levels in day-9 embryos (7% of the adult AQP4 content) and increased to 16% in day-14 embryos. A strong increase occurred between day-14 and day-20 embryos when the

expression level was at a maximum, and did not change significantly in the 2-day-old chicks.

To determine the level of AQP4 mRNA, we performed quantitative RT-PCR experiments (Fig. 1D). The amount of AQP4 PCR product was analyzed together with the co-amplification of 18S RNA (488 bp), an invariant internal standard. Results showed that the AQP4 PCR (340 bp fragment) product was not detectable in day 3 embryos but by day 9 embryos AQP4 mRNA levels were already very high, and had reached 75% of the adult mRNA content.

Morphology

Chick embryo, day 9

On day 9, the wall of the optic tectum, telencephalon and cerebellum anlagen showed neither cells nor microvessels labeled by anti-AQP4 antibody (Fig. 2A). Ultrastructurally, the tectum vessels of the optic tectum appeared to be built up with irregular endothelium together with numerous vesicles and vacuoles. The plasma membranes of adjacent endothelial cells were simply apposed, and tight interendothelial junctional systems were not recognizable. Short expansions of pericytes were found beneath the endothelial cells, whereas a basal lamina was not recognizable. Large perivascular spaces and processes of neuroblasts surrounded these primordial microvessels (Fig. 2B,C). Immunogold electron microscopic detection of AQP4 did not label vessels and neuropile (Fig. 2D).

Chick embryo, day 14

On day 14, faint AQP4 expression was detectable in the optic tectum, telencephalon and cerebellum.

Labeled bodies and processes of astroglial cells, either scattered in the neuropile or near the vessels were found. The glia *limitans* membrane, composed of endfeet of radial glia fibers and astrocyte processes, as well as the microvessels penetrating the nervous wall appeared labeled (Fig. 3A,B). The neural epithelium lining the ventricular cavities showed labeled cells alternating with unlabeled ones (Fig. 3C). A discontinuous AQP4 positivity was present around the vessels of the deeper layers of the tectum and telencephalon and cerebellum, where bodies and processes of astroglial cells, discontinuously encircling the vascular wall, were marked (Figs 3D,E, 5A). Neuroblasts and meningeal membranes were not stained.

Ultrastructurally, the tectum microvessels appeared to be lined by endothelial cells that were irregular in thickness, sealed by short tight junctions, and subtended by discontinuous basal lamina and pericytic processes. Isolated perivascular glial endfeet, filled with glycogen granules, discontinuously adhered to the vessel wall; small perivascular spaces were still present (Fig. 4A). On the replicas, small aggregates of OAPs, irregularly shaped and of varying sizes, were recognizable on the P-faces of the perivascular astrocyte membranes. Single linear chains of intramembrane particles (IMPs) were found on the membranes together with the OAPs (Fig. 4B).

On ultrathin sections, AQP4 immunoreactivity was localized on the plasma membranes of the astrocyte bodies and processes discontinuously enveloping the vessel wall, where isolated or clustered gold particles were recognizable.

Chick embryo, day 20

On day 20, the cyto- and myelo-architecture of the tectum,

telencephalon and *cerebellum* were completely developed as well as their vessel pattern.

After AQP4 immunoreaction, the tectum and telencephalon showed strong positivity of bodies and processes of astrocytes distributed in all the nervous wall layers. The ependymal cells and the microvessel abluminal sides were also strongly labeled. Stained bodies and processes of perivascular astrocytes entirely enveloped the microvessels (Figs 3F,G, 5B). In the cerebellum, grey and white matter processes of astrocytes adherent to the vessel wall were AQP4-stained. Immunoreactive astrocytes were also seen scattered throughout the granular layer, whereas they were rare in the cerebellum white core. AQP4 was expressed by Bergmann glial cells, whose bodies and processes crossing the molecular layer were strongly immunostained. Neurons, including Purkinje cells, were unlabeled (Fig. 5C).

Ultrastructurally, the tectum microvessels were lined by thin endothelial cells joined by extensive tight junctions and subtended by a continuous basal lamina and pericytic processes. Astrocyte processes almost completely enveloped the microvessel wall where it was not surrounded by perivascular spaces (Fig. 4C).

On freeze-fractured specimens, OAPs larger than those found in day-14 embryos could be identified on the perivascular astroglial membranes (Fig. 4E).

After postembedding immunogold treatment on ultrathin sections, numerous gold particles, arranged singularly or in clusters, decorated the perivascular astrocytic membranes, and were more numerous on the plasma membranes facing the vessel than on those facing the neuropile (Fig. 4G).

Newly hatched chicks

In the optic tectum, telencephalon and cerebellum of newly hatched chicks, AQP4 staining did not differ from that of the day-20 embryos. Astrocytic processes strongly positive for AQP4 formed a dense network throughout the neuropile and a continuous sheath around the vessels. Ependymal cells were also strongly marked; their basal processes and those of

Fig. 4. Ultrastructural features in day-14 embryos (A,B), day-20 embryos (C,E,G) and 2-day-old chicks (D,F). (A) Microvessel wall composed of endothelial cells with short tight junctions (arrow) and pericytes (p) is discontinuously surrounded by isolated astroglial endfeet (arrowheads). Narrow perivascular spaces (asterisks) are recognizable. (B) Replica from a fractured microvessel showing the P-face of the plasma membrane of an astrocytic endfoot with aligned individual IMPs (arrowhead) and small quadrangular OAPs (circles). (C) A continuous layer of glial endfeet filled with glycogen granules (arrowheads) surrounds the basal lamina of a microvessel lined by a thin endothelium (e) and pericytes. (D) An extensive tight junction, with points and lines of fusion of the membrane external leaflets (arrows), seals two adjacent endothelial cells. (E,F) Replicas from fractured microvessels showing E-faces of perivascular astroglial endfeet with a number of assembly pits with orthogonal symmetry (circles) corresponding to OAPs of the P-face. The assemblies are more numerous in the chick (F) than in the embryos (E). (G) Ultrastructural immunodetection of AQP4: numerous immunogold particles, arranged singularly (arrowheads) or in clusters (arrows), decorate the plasma membranes of the astroglial endfeet (g) facing the vessel endothelium. Note the unlabeled endothelial cells (e) joined by a tight junction (asterisk). Scale bars, 0.5 μm (A); 0.05 μm (B); 1.04 μm (C); 0.08 μm (D); 0.05 μm (E); 0.052 μm (F); 0.15 μm (G).

astrocytes located in the tectum deep layer formed sheaths to the microvessels of the periventricular plexus (Fig. 3H).

The ultrastructural features of the microvessels were similar to those shown by the day-20 embryos. Mature tight junctions, with points and lines of fusion between the external plasma membrane leaflets, sealed the endothelial cells (Fig. 4D). On the replicas, the perivascular glial endfeet showed a greater number of regularly shaped assemblies, square or rectangular in shape, and built up of tightly packed particles (Fig. 4F).

On ultrathin sections, AQP4 gold particles strongly marked the perivascular glial membranes, which were not different from those in 20-day embryos.
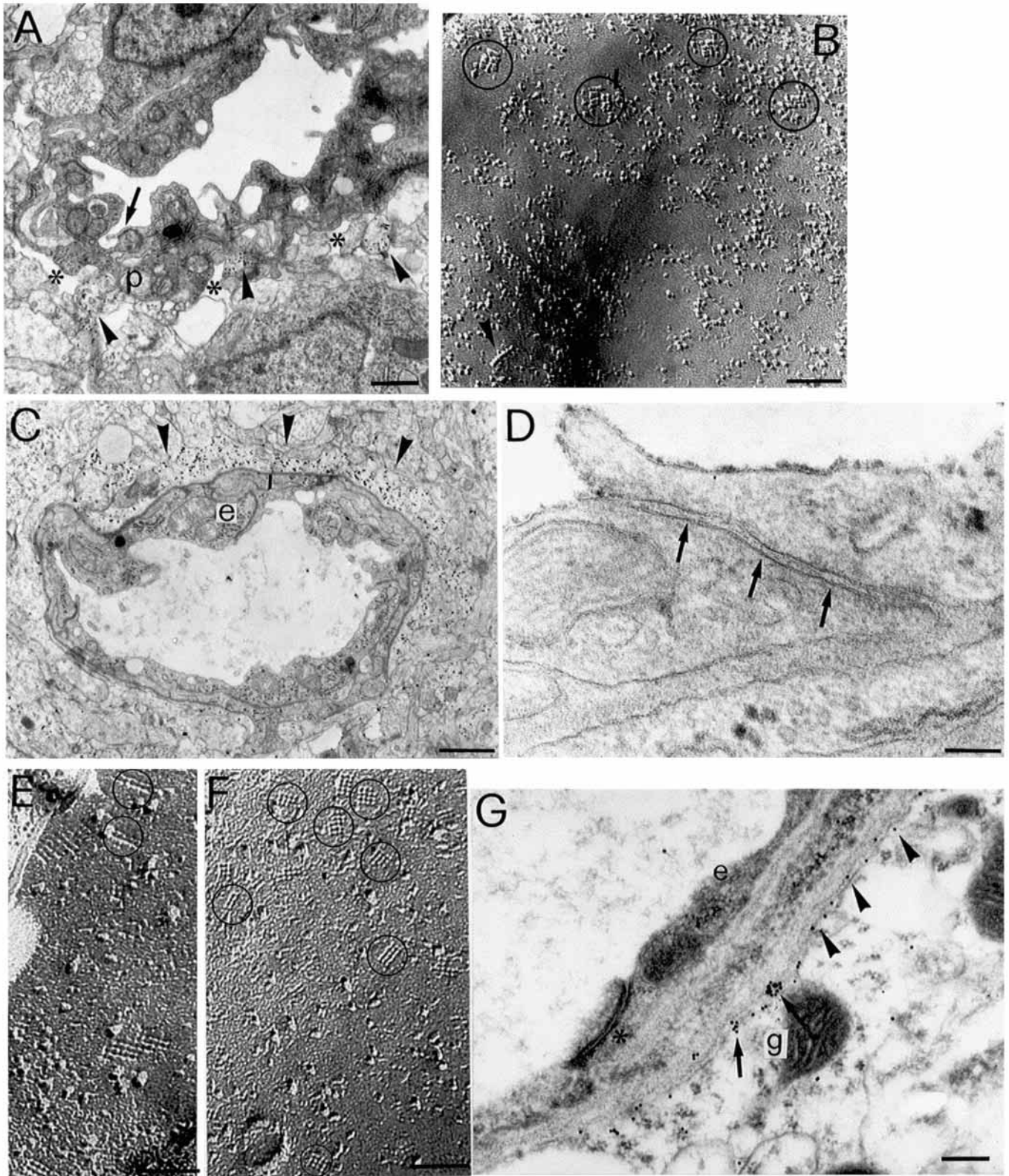
Fig. 5. (A-C) Immunohistochemical AQP4 detection in telencephalon of 14-day embryos (A) and 20-day embryos (B) and in the cerebellum of 20-day embryos. (D-H) Optic tecta of normal (D) and 20-day embryos treated with LPS (E-H). (A) Light immunopositivity of glial endfeet apposed on the abluminal side of the microvessel wall (arrow). Note that the endothelium and the neuroblasts are unstained. (B) Strong immunopositivity of glial bodies and processes surrounding a microvessel (arrows) and forming a continuous perivascular sheath (arrowhead). (C) Sagittal cerebellum section showing a heavy labeling of astrocytic processes (arrow) surrounding a microvessel in the molecular layer (m), and apposed to Purkinje cells (arrowhead). Note the unlabeled cytoplasms of the Purkinje cells (p), and the staining of astrocytic processes running in the neuropile of the molecular and granular layers (g). (D) Optic tectum wall of a control embryo showing an intravascular localization of the HRP reaction product; the neuropile is unlabeled. (E) Optic tectum wall of LPS-treated embryos showing numerous perivascular areas of HRP diffusion in the neural substratum (arrows). (F,G) Ultrathin sections showing swollen glial endfeet (F, asterisks) around the vascular wall, and an altered tight junction with detachment of the apposed plasma membrane leaflets (G, arrowheads). (H,I) AQP4 immunodetection in the tectum wall of LPS-treated embryos. A faint staining can be seen in the astrocytic processes running in the neural substratum and investing the vessel wall (H inset, arrowheads). Compare with F and G of Fig. 3. (I) Rare AQP4 gold particles (arrows) on the swollen glial endfeet (asterisks) facing a vessel. Compare with G of Fig. 4. Scale bars, 12.5 μm (A); 30 μm (B); 15 μm (C); 120 μm (D); 50 μm (E); 0.7 μm (F); 0.2 μm (G); 50 μm (H; inset, 10 μm); 0.2 μm (I).
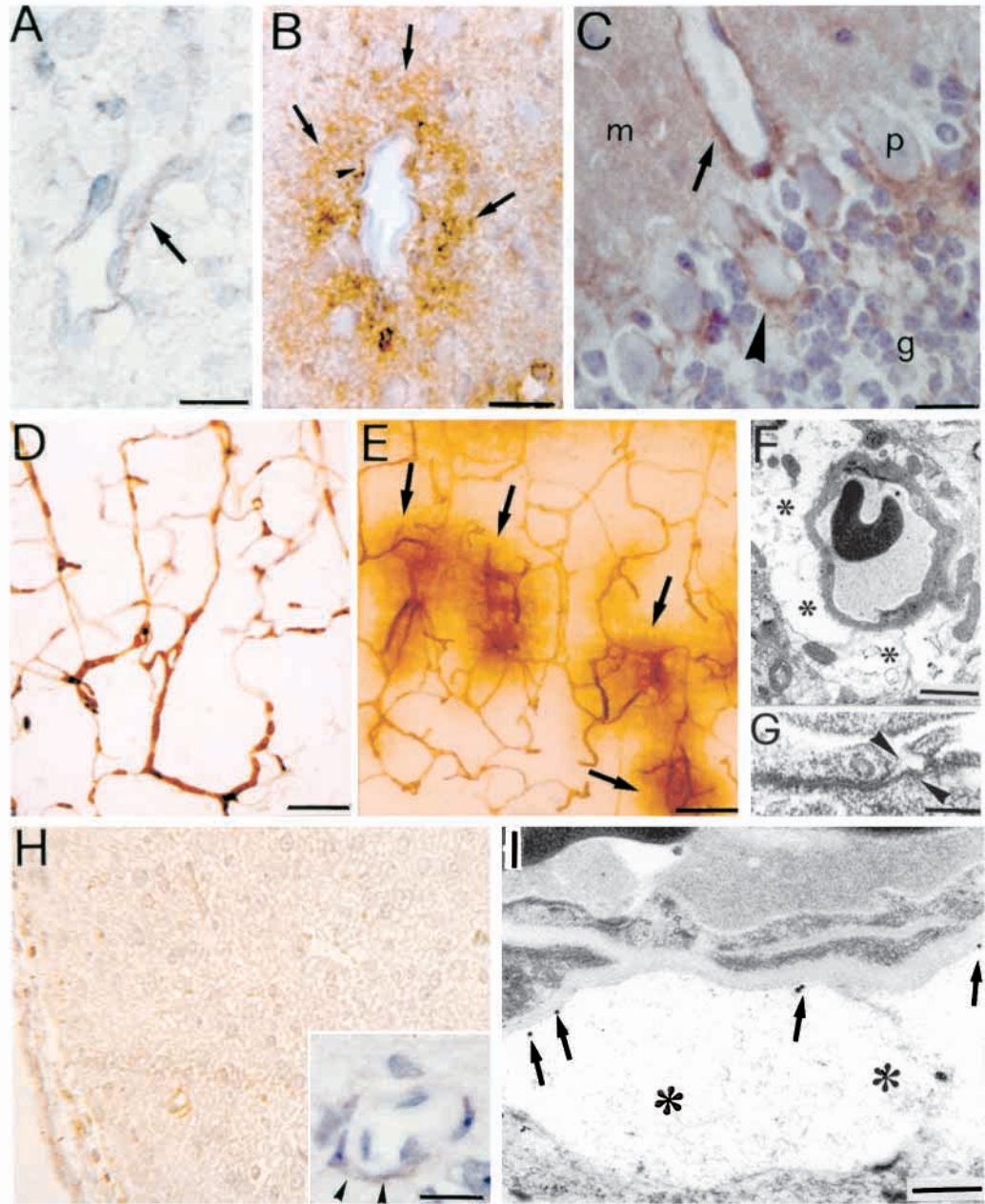
LPS effect on the BBB integrity and glial AQP4 expression

The BBB of the optic tectum of the 20-day embryos treated with LPS showed remarkable differences when compared to that of the control. After HRP injection, numerous and extensive perivascular areas of HRP escape were observed by light microscopy (Fig. 5E), and these were different from the control tectum, where the permeability marker was exclusively localized in the vessel lumina (Fig. 5D). Ultrastructurally, the microvessel walls of the LPS-treated embryos showed irregular endothelium, with more vesicles and vacuoles. The endothelial cells were sealed by modified tight junctions, owing to microdetachments between the apposed plasma membrane leaflets (Fig. 5G). The glial endfeet surrounding the vascular wall were swollen and devoid of glycogen granules (Fig. 5F). After AQP4 immunoreaction, the tectum of the embryos treated with LPS showed a faint labeling of the astrocytic processes distributed in the neuropile and arranged around the microvessels. These processes appeared faintly and discontinuously stained, alternating labeled regions with unlabeled ones (Fig. 5H, insert). After immunogold reaction, a few AQP4 gold particles were found on the glial endfoot plasma membranes facing the microvessels of the LPS-treated embryos treated with LPS (Fig. 5I).

DISCUSSION

The present study demonstrates for the first time that expression of the AQP4 water channel in the brain is largely embryonal and developmentally regulated during the BBB maturation.

In contrast to Wen and coworkers, who observed only a postnatal AQP4 expression in the rat cerebellum (Wen et al., 1999), we demonstrate the expression of AQP4 water channels during early embryonic development, by ependymoglial cells of the neural epithelium and astroglia lineage cell bodies and processes forming the limiting membrane and investing the vascular walls of the chick optic tectum, telencephalon and cerebellum.

This discrepancy might reflect the fact that the chick brain is much more mature at the end of the embryonic development than that of the rat (Horstmann, 1959). This statement is confirmed by the evidence of a precocius cerebral electrical activity in avian embryos, and of their capacity to respond to various external stimuli (Peters et al., 1965; Peters et al., 1973; Corner et al., 1966). Moreover, while in the rat maximal cerebral capillary proliferation occurs only in postnatal life (Robertson et al., 1985), in the avian brain angiogenetic processes are complete by the end of the embryonic life (Roncali et al., 1986). In this context, our observations on AQP4 embryonic expression in the chick brain might be related to its precocious differentiation.

We could not detect AQP4 expression in the brain of day-9 embryos by immunocytochemistry, whereas the immunoblotting results do show small amounts of AQP4. This difference might be the result of the higher sensitivity of the immunoblot technique, or because the first astroglial cells appearing early in the CNS have only a low content of AQP4 protein, which is diffused within the cytoplasm instead of being incorporated in the plasma membranes.

PCR analysis revealed high AQP4 mRNA levels in day-9 embryos, indicating that the AQP4 gene is activated early on during avian brain embryonic development. In contrast, the protein level is first detectable on day 9 and reaches a maximum in day-20 embryos. It therefore seems conceivable that, during the CNS brain maturation, the protein expression pattern follows the glia development pattern.

Histochemical AQP4 expression is first recognizable in the chick brain microvasculature of day-14 embryos, and the highest AQP4 expression is revealed in day-20 embryos, when the microvessels are enveloped by a continuous astroglial sheath, and provided with mature barrier devices (Nico et al., 1997; Nico et al., 1998; Nico et al., 1999).

It is worth stressing the relationships occurring between perivascular space reduction and AQP4 expression during development. It is well known that remarkable amounts of fluid move across epithelial and endothelial barriers in prenatal life. It is also generally accepted that the last days of development are characterized by body mass increase, due to both a high rate of cell proliferation and a reduction of extracellular space volume, in turn depending upon water flux regulation (Caley and Maxwell, 1970; Lehmenkuhler et al., 1993). In the early embryo brain, in particular, large extracellular spaces allow the free diffusion of water and ions from permeable vessels that are not ensheathed by glia (Risau, 1989; Lossinsky et al., 1986). In subsequent development, when endfeet of astroglial processes are being arranged around the vessel walls and the BBB is differentiating, the perivascular spaces are drastically reduced, owing to a series of mechanisms involving both exclusion and active taking up of substances from the blood stream (Betz and Goldstein, 1986; Bertossi et al., 1993; Nico et al., 1997).

The detection of AQP4 protein in the chick embryo tectum simultaneously with the formation of a perivascular sheath of astroglial endfeet therefore suggests that the regulation of the water transport, probably associated with K^+ flux generated by neural activity (siphoning), is controlled by specific water channels, which have already appeared in the perivascular astroglia during embryonic development.

In addition, the results indicate that the astrocyte involvement in the water flux control and tightening of the endothelial barrier are closely related developmental events, leading together to the complex setting up of the BBB.

Interestingly, we have found that the AQP4 developmental expression increases parallel to the formation of the OAPs, recognized by freeze-fracture techniques in the plasma membranes of several cell types, including ependymal cells and astrocytes enveloping blood vessels (Landis and Reese, 1981; Neuhaus et al., 1990). OAP formation takes place through the transformation of short chains of IMPs into orthogonal aggregates, which are smaller in embryonic than in mature astrocytes (Nico et al., 1994). The identity and function of OAPs are not completely known. In mature astrocytes, OAPs are associated with K^+ siphoning, and recent data indicate that they are formed by clusters of AQP4 molecules (Yang et al., 1996; Verbavatz et al., 1997; Rash et al., 1998). In the present study, use of AQP4 immunogold staining and freeze fracture techniques in parallel allowed us to demonstrate that AQP4 expression and OAP maturation on the perivascular glia membranes follow the same temporal sequence. These observations strongly corroborate the finding that AQP4 protein is involved in the molecular composition of the OAPs, thus attributing to them a role in the control of the water flux that takes place during brain embryogenesis.

Our results further emphasize the key role that the astrocytes play in the development, function and maintenance of the BBB, not only by the induction of morphological and biochemical devices in the endothelial cells of the cerebral vasculature but also by regulation of the water flux involved in the CNS homeostasis. In normal conditions, astrocytes form a continuous sheet around the vessels, and maintain cerebral homeostasis through direct or indirect action on endothelial cells by regulating the ionic flux occurring during neuronal activity (Sun et al., 1995). We have demonstrated that the glial regulation of the water balance starts in embryonic life and is coupled with BBB functionality. When the BBB is altered by LPS treatment, brain oedema occurs, the glial astrocytes are swollen and display a strong reduction of AQP4 protein. This evidence agrees with the commonly accepted statement that astrocytic swelling is a cell reaction to BBB injury and, in turn, expression of the failure of ion homeostasis.

Therefore, in our study, reduced glial AQP4 expression on swollen glial endfeet, together with a failure in BBB, indicate a close relationship between BBB functioning and control of water flux by astroglial cells, and suggest an important involvement of this protein in the determining of the brain oedema, in adult and embryonic life.

The hypothesis that AQP4 protein has a developmental role

in the regulation of the cerebrospinal fluid (CSF) by ependymal cells is also supported by our results. We have previously demonstrated in adult animals that AQP4 ependymal expression correlates with CSF reabsorbtion (Frigeri et al., 1995a; Frigeri et al., 1995b) whereas CSF formation has been associated with the expression of the water channel AQP1 by the choroid plexus cells (Nielsen et al., 1993). The initial AQP4 expression shown by the epithelial cells lining the tectum ventricle in day-14 embryos and the increment of the protein expression in day-20 embryos, agrees with the concept that the AQP4 water channel may intervene in the CSF reabsorbtion during CNS morphohistogenesis.

In conclusion, the presence of specific sites of expression of AQP4 protein in embryonic astroglia and ependymoglia is strongly consistent with the suggestion that these cells play a control role in the fluid transport by a water channel that is early expressed, developmentally regulated and tightly associated with the BBB integrity. Finally, the early developmental expression of AQP4 suggests, at least in the avian species, the existence of a close relationship between water transport regulation and brain development.

REFERENCES

Agre, P., Bonhivers, M. and Borgnia, M. J. (1998). The aquaporins, blueprints for cellular plumbing system. *J. Biol. Chem.* **273**, 14659-14662.

Beck, D. W., Vinters, H. V., Hart, M. N. and Cancilla, P. A. (1984). Glial cells influence polarity of the blood-brain barrier. *J. Neuropathol. Exp. Neurol.* **43**, 219-224.

Bertossi, M., Roncali, L., Nico, B., Ribatti, D., Mancini, L., Virgintino, D., Fabiani, G. and Guidazzoli, A. (1993). Perivascular astrocytes and endothelium in the development of the blood-brain barrier in the optic tectum of the chick embryo. *Anat. Embryol.* **188**, 21-29.

Betz, A. L. and Goldstein, G. W. (1986). Specialized properties and solute transport in brain capillaries. *Annu. Rev. Physiol.* **48**, 241-250.

Branton, D., Bullivant, S., Gilula, N. B., Karnovsky, M. J., Moor, H., Muhlethaler, K., Northcote, D. H., Packer, L., Satir, B., Satir, P., Speth, V., Staehlin, L. A., Steere, R. L. and Weinstein, R. S. (1975). Freeze-etching nomenclature. *Science* **190**, 54-56.

Caley, D. W. and Maxwell, D. S. (1970). Development of the blood vessels and extracellular spaces during postnatal maturation of rat cerebral cortex. *J. Comp. Neurol.* **138**, 31-48.

Cancilla, P. A. and DeBault, L. E. (1983). Neutral amino acids transport properties of cerebral endothelial cells in vitro. *J. Neuropathol. Exp. Neurol.* **42**, 191-199.

Corner, M. A., Peters, J. J. and Loeff, P. R. Van Der (1966). Electrical activity patterns in the cerebral hemisphere of the chick during maturation, correlated with behaviour in a test situation. *Brain Res.* **2**, 274-292.

DeBault, L. E. and Cancilla, P. A. (1980). Gamma glutamyl transpeptidase in isolated brain endothelial cells: induction by glial cells in vitro. *Science* **207**, 653-655.

Frigeri, A., Gropper, M. A., Turck, C. W. and Verkman, A. S. (1995a). Immunolocalization of the mercurial-insensitive water channel and glycerol intrinsic protein in epithelial cell plasma membranes. *Proc. Natl. Acad. Sci. USA* **92**, 4328-4331.

Frigeri, A., Gropper, M. A., Umenishi, F., Kawashima, M., Brown, D. and Verkman, A. S. (1995b). Localization of MIWC and GLIP water channel homologs in neuromuscolar epithelial and glandular tissue. *J. Cell Sci.* **108**, 2993-3002.

Frigeri, A., Nicchia, G. P., Verbavatz, J. M., Valenti, G. and Svelto, M. (1998). Expression of Aquaporin-4 in Fast-Twitch fibers of mammalian skeletal muscle. *J. Clin. Invest.* **102**, 695-703.

Hasegawa, H. T., Skach, M. W., Matthay, M. and Verkman, A. S. (1994). Molecular cloning of a mercurial-insensitive water channel expressed in selected water transporting tissues. *J. Biol. Chem.* **269**, 5497-5500.

Horstmann, E. (1959). Die postnatale Entwicklung der kapillarisierung im Gehirn eines Nesthockers (Ratte) und eines Nestfluchters (Meerschweinchen). *Anat. Anz.* **106/107**, 405-410.

Janzer, R. C. and Raff, M. (1987). Astrocytes induce blood-brain barrier properties in endothelial cells. *Nature* **325**, 253-257.

Jung, J. S., Bhat, R. V., Preston, G. M., Guggino, W. B., Baraban, J. M. and Agre, P. (1994). Molecular characterization of an aquaporin cDNA from brain: candidate osmoreceptor and regulator of water balance. *Proc. Natl. Acad. Sci. USA* **91**, 13052-13056.

King, L. S., Nielsen, S. and Agre, P. (1997). Aquaporins in complex tissue. I. Developmental patterns in respiratory and glandular tissues of rat. *Am. J. Physiol.* **273**, 2183-2191.

Landis, D. M. D. and Reese, T. S. (1981). Membrane structure in mammalian astrocytes: A reviw of freeze-fracture studies on adult, developing, reactive and altered astrocytes. *J. Exp. Biol.* **95**, 35-48.

Lehmenkuhler, A., Sykovà, E., Svoboda, J., Zilles, K. and Nicholson C. (1993). Extracellular space parameters in the rat neocortex and subcortical white matter during postnatal development determined by diffusion analysis. *Neuroscience* **55**, 339-351.

Lossinsky, A. S., Vorbrodt, A. W. and Wisniewski H. M. (1986). Characterization of endothelial cell transport in the developing mouse blood-brain barrier. *Dev. Neurosci.* **8**, 61-75.

Markwell, M. A., Haas, S. M., Bieber, L. L. and Tolbert, N. E. (1978). A modification of the Lowry procedure to simplify protein determination in membrane and lipoprotein samples. *Anal. Biochem.* **87**, 206-210.

Meresse, S., Dehouck, M. P., Delorme, P., Bensaid, M., Tauber, J. P., Delbart, C., Fruchart, J. C. and Cecchelli, R. (1989). Bovine brain endothelial cells express tight junctions and monoamine oxidase activiy in long-term culture. *J. Neurochem.* **53**, 1363-1371.

Nagelhus, E. A., Veruki, L. M., Torp, R., Haug, F. M., Laake, J. H. and Nielsen, S. (1998). Aquaporin-4 water channel protein in the rat retina and optic nerve: polarized expression in Muller cells and fibrous astrocytes. *J. Neurosci.* **18**, 2506-2519.

Nagelhus, E. A., Horio, Y., Inanobe, A., Fujita, A., Haugh, F. M., Nielsen, S., Kurachi, Y. and Ottersen, P. (1999). Immunogold evidence suggests that coupling of K^+ siphoning and water transport in rat retinal Muller cells is mediated by a coenrichment of Kir 4.1 and AQP4 in specific membrane domains. *Glia* **26**, 47-54.

Neely, J. D., Christensen, B. M., Nielsen, S. and Agre, P. (1998). Heterotetrameric composition of aquaporin-4 water channels. *Biochemistry* **38**, 1156-1163.

Neuhaus, J. (1990). Orthogonal array of particles in astroglial cells: quantitative analysis of their density, size and correlation with intramembrane particles. *Glia* **3**, 241-245.

Newman, E. A. (1995). Glial regulation of extracellular potassium. In *Neuroglia* (ed. H. Kettenman and B. R. Ramson), pp. 717-731. New York: Oxford University Press.

Nicchia, P., Frigeri, A., Liuzzi,G. P., Santacroce, M. P., Nico, B., Procino G., Quondamatteo, F., Herken, R., Roncali, L. and Svelto, M. (2000). Aquaporin-4 containing astrocytes sustain a temperature and mercury-insensitive swelling in vitro. *Glia* **31**, 29-38.

Nico, B., Cantino, D., Sassoè-Pognetto, M., Bertossi, M. and Roncali, L. (1994). Orthogonal array of particles (OAPs) in perivascular astrocytes and tight junctions in endothelial cells. A comparative study in developing and adult brain microvessel microvessels. *J. Submicrosc. Cytol. Pathol.* **26**, 193-109.

Nico, B., Cardelli, P., Fiori, A., Riccetelli, L., Giglio, R. M., Strom, R., Sassoè-Pognetto, M., Cantino, D., Bertossi, M., Ribatti, D. and Roncali, L. (1997). Developmental study of ultrastructural and biochemical changes in isolated chick brain microvessels. *Microvasc. Res.* **53**, 79-91.

Nico, B., Quondamatteo, F., Ribatti, D., Bertossi, M., Russo, G., Herken, R. and Roncali, L. (1998). Ultrastructural localization of lectin binding sites in the developing brain microvasculature. *Anat. Embryol.* **197**, 305-315.

Nico, B., Quondamatteo, F., Herken, R., Marzullo, A., Corsi, P., Bertossi, M., Russo, G., Ribatti, D. and Roncali, L. (1999). Developmental expression of ZO-1 antigen in the mouse blood-brain barrier. *Dev. Brain Res.* **114**, 161-169.

Nielsen, S., Smith, B. L., Christensen, E. I. and Agre, P. (1993). Distribution of aquaporin CHIP in secretory and resorptive epithelia and capillary endothelia. *Proc. Natl. Acad. Sci. USA* **90**, 7275-7279.

Nielsen S. and Agre, P. (1995). The aquaporin family of water channels in kidney. *Kidney Int*. **48**, 1057-1068.

Nielsen, S., Nagelhus, E. A., Amiry-Moghaddam, M., Bourque, C. and Agre, P. (1997). Specialized membrane domains for water transport in glial cells: high resolution immunogold cytochemistry of aquaporin-4 in rat brain. *J. Neurosci*. **17**, 171-180.

Pardridge, W. M. (1988). Recent advances in blood-brain barrier transport. *Annu. Rev. Pharmacol. Toxicol.* **28**, 25-39.

Peters, J., Vonderahe, A. R. and Schimd, D. (1965). Onset of cerebral electrical activity associated with behavioral sleep and attention in the developing chick. *J. Exp. Zool* **160,** 255-261.

Peters, J., Hilgeford, E. J. and Vonderahe, A. R. (1973). Ontogenesis of electroencephalographic seizure patterns in developing chick embryos during recovery from hypothermic hypoxia. *Dev. Psychobiol*. **6**, 337-348.

Quagliarello, V. J., Long, W. J. and Scheld, W. M. (1986). Morphologic alteration of blood-brain barrier with experimental meningitis in the rat. Temporal sequence and role of encapsulation. *J. Clin. Invest*. **77**, 1084-1095.

Rash, J. E., Yasumara, T., Hudson, C. S., Agre P. and Nielsen, S. (1998). Direct immunogold labeling of aquaporin-4 in square arrays of astrocyte and ependymocyte plasma membranes in rat brain and spinal cord. *Proc Natl. Acad. Sci. USA* **95**, 11981-11986.

Raub, T. J., Kuentzel, S. L. and Sawada, G. A. (1992). Permeability of bovine brain microvessel endothelial cells in vitro. Barrier tightening by a factror released from astroglioma cells. *Exp. Eye Res*. **199**, 330-340.

Reese, T. S. and Karnowsky, M. J. (1967). Fine structural localization of a blood-brain barrier to exogenous peroxidase. *J. Cell Biol*. **34**, 207-217.

Risau, W. (1989). Differentiation of the blood-brain barrier endothelium. *News Physiol. Sci.* **4**, b151-153.

Risau, W. and Wolburg, H. (1990). Development of the blood-brain barrier. *Trends Neurosci.* **13**,174-178.

Robertson, P. L., Du Bois, M., Bowman, P. D. and Goldstein, G. W. (1985). Angiogenesis in developing rat brain: An in vivo and in vitro study. *Dev. Brain Res*. **23**, 219-223.

Roncali, L., Nico, B., Ribatti, D., Bertossi, M. and Mancini, L. (1986). Microscopical and ultrastructural investigations on the development of the blood-brain barrier in the chick embryo optic tectum. *Acta Neuropathol*. **70**, 193-201.

Rubin, L. L, Hall, D. E., Porter, S., Barbu, K., Cannon, C., Horner, H. C.,

Janatpour, M., Liaw, C. W., Manning, K., Morales, J., Tanner, L. J., Tomaselli, K. J. and Bard, F. (1991). A cell culture model of the blood-brain barrier. *J. Cell Biol*. **115**, 1725-1736.

Saunders, N. R. (1977). Ontogeny of the blood-brain barrier. *Exp. Eye Res.* **25S**, 523-550.

Schulze, C. and Firth, A. J. (1992). Interendothelial junctions during blood-brain barrier development in the rat: morphological changes at the level of individual tight junctional contacts. *Dev. Brain Res*. **69**, 85-95.

Sun, D., Lytle, C. and O'Donnel, M. (1995). Astroglial cell-induced expression of Na-K-Cl cotransporter in brain microvascular endothelial cells. *Am. J. Physiol.* **269**C, 1506-1512.

Tao-Cheng, J. H., Nagy, Z. and Brightman, M. W. (1987). Tight junctions of brain endothelium in vitro are enhanced by astroglia. *J. Neurosci*. **7**, 3293-3299.

Tunkel, A. R., Rosser, S. W., Hansen, E. J., Scheld, W. M. (1991). Blood-brain barrier alterations in bacterial meningitis. Development of in vitro model and observations of the effects of lipopolysaccharide. *In Vitro Cell Dev. Biol.* **27A**, 251-261

Verkman, A. S., Van Hoeck, A. N., Tonghui, MA., Frigeri, A., Schach, W. R., Mitra, A., Tamarappoo, B. K. and Farinas, J. (1996). Water transport across mammalian cell membranes. *Am. J. Physiol*. **39**, C12-C30.

Verbavatz, J. M., Tonghui, M. A., Gobin, R. and Verkman, A. S. (1997). Absence of orthogonal arrays in kidney, brain, and muscle, from transgenic knockout mice lacking water channel aquaporin-4. *J. Cell Sci*. **110**, 2855-2860.

Yang, B., Brown, D. and Verkman, A. S. (1996). The mercurial-insensitive water channel (AQP4) forms orthogonal arrays in stably transfected CHO cells. *J. Biol. Chem.* **271**, 4577-4580.

Wakai,S. and Hirokawa, N. (1978). Development of the blood-brain barrier to horseradish peroxidase in the chick embryo. *Cell Tiss. Res*. **195**, 195-203

Walz, W. and Hinks, E. C. (1985). Carrier-mediated KCl accumulation accompanied by water movements is involved in the control of physiological K+ levels by astrocytes. *Brain Res*. **343**, 44-51.

Wen, H., Nagelhus, E. A., Amiry-Moghaddam, M., Agre, P., Ottersen, O. P. and Nielsen, S. (1999). Ontogeny of water transport in rat brain: postnatal expression of the aquaporin-4 water channel. *Eur. J. Neurosci*. **11**, 935-994.

Wilspelwey, B., Lesse, A. J., Hansen E. J. (1988) *Haemophilus influenzae* lipopolysaccharide-induced blood-brain barrier permeability during experimental meningitis in the rat. *J. Clin. Invest*. **82**, 1339-1346